Active Control of Nonlinear Disturbances in 2-D Boundary Layers

C. Gmelin, U. Rist, S. Wagner
Universität Stuttgart, Institut für Aerodynamik und Gasdynamik
Pfaffenwaldring 21, D-70550 Stuttgart, Germany

Summary

The purpose of the current investigation is the development of techniques which allow the active control of disturbances occurring in transitional boundary layers. Due to the inability of techniques following the wave-superposition principle to damp nonlinear high-amplitude disturbances we favour an approach called ω_z-*control*. It is shown, that the direct feedback of instantaneous flow signals from the wall is well suited to drive the active control without additional control loops between sensor and actuator. In our case the spanwise vorticity (ω_z) or its first streamwise derivative on the wall is sensed, multiplied by a certain factor A and prescribed as a new boundary condition at the wall with some time delay Δt. Investigations using Linear Stability Theory (LST) show a strong dependence of achieved damping rates from the phase between $\omega_{z,w}$ and wall-normal velocity v_w. With a properly adjusted phase even in very unstable base-flows (e.g. with adverse pressure gradient) a remarkable transition delay can be achieved. With aid of Direct Numerical Simulation (DNS) different transition scenarios have been simulated to confirm the LST-results and to study the active control of high amplitude disturbances in stages of transition where nonlinear interactions have already set in.

1 Introduction

In times of emerging fuel costs there is a strong interest in concepts to actively control the laminar-turbulent transition with the goal to reduce skin friction. In contrast to using the wave superposition principle [1] new approaches appeared, directly modifying the modal structure of the influenced disturbances. One of these methods is the ω_z-*control* which is, in contrast to wave superposition methods, able to reduce even nonlinear disturbances near the final transition to turbulence. In this case no kind of "anti-disturbance" is overlaid but wavenumber and amplification rate of existing eigenfunctions are changed significantly (cf. section 3).

*Proceedings of the DRAG-NET Conference, June/2000, Potsdam

Two different base flows are considered: a Blasius and a Falkner-Skan boundary layer with adverse pressure gradient (Hartree parameter is $\beta_H = -0.1$). Besides extensive investigations using LST the behaviour of nonlinear disturbances leading to a K-breakdown in a Blasius boundary layer is examined using spatial DNS (cf. section 5).

2 Control Principle

To damp disturbances in boundary layers we use the feedback of instantaneous signals of the spanwise vorticity measured at the wall. These signals are multiplied by an amplitude factor $|A|$ and are prescribed as a v-boundary condition after a time delay Δt at the wall which is necessary to produce the phase shift Θ shown in Fig.1 a).

Investigations (see section 3) using LST showed, that control is most effective for the case of $\Theta = \frac{\pi}{2}$, i.e. a phase shift of 90 degrees which can also be achieved by setting v_w proportional to $\frac{\omega_z}{x}$. To eliminate the inherent instability of the altered procedure a modified control algorithm was developed:

$$v_w = \frac{\partial \omega_{z,w}}{\partial x} \cdot \frac{|\omega_{z,w}|_{max}}{|\frac{\partial \omega_{z,w}}{\partial x}|_{max}} \cdot |A| \tag{1}$$

The maxima in eqn. 1 are each calculated over approximately one wavelength up- and downstream. This algorithm is able to produce a control signal proportional to the first derivative of $\omega_{z,w}$ whose amplitude is always lower than $|A| \cdot \omega_{z,w}$. A detailed discussion of the underlying physical mechanisms can be found in [3]. In contrast to approaches based on the superposition of disturbances with opposite phase working with linear transfer functions between sensor and actuator like the FIR-filter concept (Fig.1 b), for details see [4]), no downstream transport of information has to be modeled here. Furthermore, there is no need of an error sensor located far downstream to tune control parameters, it represents a pure feed-forward approach.

3 Results of the Linear Stability Theory

To study the behaviour of linear instability waves under the influence of active ω_z-control investigations using LST were undertaken. Therefore, the boundary conditions at the wall for the Orr-Sommerfeld (and Squire equation) had to be changed (index w denotes wall properties) to

$$\begin{aligned} v_w &= A \cdot \omega_{z,w} \\ \text{with} \quad A &= |A| \cdot e^{i\Theta} \quad , \end{aligned} \tag{2}$$

where $|A|$ is the amplitude factor and Θ is the phase difference between v_w and $\omega_{z,w}$ similar to the time delay used in the simulations. Fig.2 shows the influence of active control on the unstable area in the stability diagram of the two scenarios we looked at. For the Blasius case (a) already small amplitudes are sufficient for a strong damping effect. If the amplitude factor $|A|$ is larger than approximately $5 \cdot 10^{-5}$ for a phase angle of $\Theta = 0$ no unstable area is present

any more. For the Falkner-Skan base flow with adverse pressure gradient (b) even with large amplitudes only small decay of the disturbances is achievable. Only a proper phase shift of $\Theta \approx \frac{\pi}{2}$ yields a remarkable damping effect due to the stronger instability of the Falkner-Skan base flow. Detailed investigations concerning the dependence of the eigenvalues on the phase angle (Fig.3) show that even for the Falkner-Skan case attenuation can be reached only for a very narrow Θ-range (hatched areas in Fig.3 a) and b)). This leads directly to the necessity to adjust Θ to approximately 90 degrees and to the development of the modified control algorithm already mentioned above. Although the introduction of a phase shift in the Blasius case is not obligatory to achieve positive effects even in this case active control can be improved by applying the new control law.

4 Numerical Method

To investigate the behaviour of nonlinear waves in the Blasius-boundary layer a number of calculations using Direct Numerical Simulation (DNS) were undertaken. All simulations were performed in a rectangular integration domain with the spatial DNS-code developed by Konzelmann, Rist and Kloker [5][6][7]. The flow is split into a steady 2D-part (base flow) and an unsteady 3D-part. The x-(streamwise) and y-(wall-normal) directions are discretized with finite differences of fourth-order accuracy and in the spanwise direction z a spectral Fourier representation is applied. Time integration is performed by the classical fourth-order Runge-Kutta scheme. The utilized variables are normalized with $\tilde{U}_\infty = 30\frac{m}{s}$, $\tilde{\nu} = 1.5 \cdot 10^{-5}\frac{m}{s^2}$ and $\tilde{L} = 0.05m$ ($\tilde{}$ denotes dimensional variables):

$$x = \frac{\tilde{x}}{\tilde{L}} \quad , \qquad y = \frac{\tilde{y}}{\tilde{L}} \quad , \qquad z = \frac{\tilde{z}}{\tilde{L}} \quad , \qquad t = \tilde{t} \cdot \frac{\tilde{U}_\infty}{\tilde{L}} \quad ,$$
$$u = \frac{\tilde{u}}{\tilde{U}_\infty} \quad , \qquad v = \frac{\tilde{v}}{\tilde{U}_\infty} \quad , \qquad w = \frac{\tilde{w}}{\tilde{U}_\infty} \quad , \qquad Re = \frac{\tilde{U}_\infty \tilde{L}}{\tilde{\nu}} = 10^5 \quad ,$$

where u, v and w are the components of the unsteady velocity disturbances. This leads to the dimensionless frequency $\beta = \frac{2\pi \tilde{f} \tilde{L}}{\tilde{U}_\infty}$, where $\tilde{f}$ is the frequency in $[Hz]$ and the dimensionless spanwise vorticity $\omega_z = \frac{\partial u}{\partial y} - \frac{\partial v}{\partial x}$.

5 DNS Results for Nonlinear Disturbances

As a test case for the effect of the ω_z-approach on disturbances with large amplitude a typical K-breakdown scenario (dotted lines in Fig.5) is used where a fundamental mode (1,0) with large amplitude and a stationary 3D-disturbance (0,1) (the first index denotes multiples of the frequency β, the second multiples of the basic spanwise wave number $\gamma = 20$) are excited initially. Because of nonlinear interactions the 3D-mode (1,1) arises and falls in resonance with the fundamental 2D-mode (modes (1,0) and (1,1) share the same wave number from $x \approx 3.4 \ldots 4.0$). The other modes shown appear due to higher order nonlinear combinations. They demonstrate transition to turbulence by generation of higher harmonics and the mean flow distortion (0,0). When the strongly amplified 3D-waves have reached the amplitude level of the fundamental mode,

saturation sets in and transition to turbulence takes place. Applying ω_z-control to this scenario two main control effects can be distinguished: direct damping of nonlinear disturbances and the affection of the resonant behaviour. The first is comparable to the linear case where ω_z-control is able to directly damp Tollmien-Schlichting(TS)-disturbances. When active control is applied, an immediate transport of fluctuation energy from disturbance to base flow sets in, reducing the amplitude of the present disturbances [3].

In opposition to more traditional approaches like FIR-filters active feedback of instantaneous flow data for active control is better suited to control transition even in cases when strong nonlinear interactions have already taken place. In the present concept no downstream transport of information has to be modeled. Therefore, the main reason for the failure of linear approaches is removed, the control doesn't have to "know" anything about the processes happening further upstream. Furthermore, the new concept doesn't require strictly wave like disturbances, a point which is very important in regions close to transition when the large-amplitude 2D-wave is strongly deformed due to nonlinear interactions and the growing 3D-waves, reaching similar amplitude levels.

In Fig.5 a) the effect of ω_z-control with optimized phase, using the modified control algorithm (1) is shown compared to the uncontrolled K-breakdown case. Control is applied immediately before the final breakdown to turbulence. Looking at the phase velocities of the modes (1,0) and (1,1) (Fig.6) one can see that phase-synchronization and therefore fundamental resonance has already set in. Anyhow, a strong damping effect is visible, the fundamental 2D-mode is reduced to an amplitude-level below 1% compared to the uncontrolled case and the accompanied 3D-modes follow after a short delay leaving large stationary modes (0,1) and (0,2). Fig.5 b) shows the damping capability compared to four different cases using a FIR-filter and therefore linear superposition of anti-phase waves to reduce nonlinear disturbances. Here the bars at the bottom of the picture denote the position of the control-strips (Index CS) of the different runs where disturbances with opposite phase are introduced. The FIR-cases have been discussed in detail in [4]. The achievable amplitude reduction of the FIR-concept is becoming worse in the vicinity of nonlinearity close to transition. When the control-strip is positioned at $x_{CS} = 2.42$ almost "linear" reduction is achievable whereas control fails completely when applied at $x_{CS} > 3.6$, in regions where disturbances are no longer wave-like. On the other hand, the ω_z-control is able to damp even those nonlinear 2D- and 3D-disturbances occurring just before transition sets in. With regard to the instantaneous flow data presented in Fig.4 it is possible to suppress the appearance of transitional structures like high-shear layers or Λ-vortices with control applied approximately one to two wavelengths upstream (Fig.4 a) and b)). Comparing wall-normal velocity v and pressure p at the wall (Fig.4 c)) a proportionality of v_w to $\frac{\partial p}{\partial x}$ can be distinguished, similar to investigations using compliant walls to control transition [2], implying similar control-mechanisms for both approaches.

The second effect mentioned above, the altering of the resonant behaviour can hardly be separated from the direct attenuation. From Fig.6 it is obvious, that both resonant modes (1,0) and (1,1) do not share the same wave number and phase speed any more immediately under the influence of control ($x > 3.46$) long before direct attenuation can be recognized ($x \gtrsim 3.7$, Fig.5 a)). This

indicates a disruption of resonance forced by active control due to the altered wave speeds of the dominant modes.

6 Summary

With the aid of Direct Numerical Simulations (DNS) it was possible to develop a simple, yet effective control algorithm to actively control the laminar-turbulent transition occurring in a 2D boundary layer. It combines two main effects: the direct attenuation and a reduced resonance according to an altered phase velocity of the involved modes. Calculations using Linear Stability Theory (LST) show a strong dependence of the resulting wave number and amplification rate on the chosen amplitude and phase difference between ω_z (sensed) and v_{wall} (stimulated).

It is shown that this approach works very well even close to transition where the boundary layer instabilities have reached a highly nonlinear stage. Investigation concerning the application of the ω_z-approach to more complex scenarios like wave packets eg. are under the way. Further research has to show how far transition can be shifted downstream and whether a complete relaminarisation of the flow is possible using this approach.

References

[1] M. Baumann and W. Nitsche. Investigations of active control of tollmien-schlichting waves on a wing. In R.A.W.M. Henkes and J.L. van Ingen, editors, *Transitional Boundary Layers in Aeronautics*, volume 46, pages 89–98. KNAW, Amsterdam, North Holland, 1996.

[2] C. Davies. *Evolution of Tollmien-Schlichting Waves Over a Compliant Panel.* PhD thesis, University of Warwick, 1995.

[3] C. Gmelin and U. Rist. Active control of laminar-turbulent transition using instantaneous vorticity signals at the wall. *to appear in Phys. Fluids*, 2000.

[4] C. Gmelin, U. Rist, and S. Wagner. Dns of active control of disturbances in a blasius boundary layer. In H. Fasel and W. Saric, editors, *Laminar-Turbulent Transition.* Springer Verlag, Berlin Heidelberg, 2000. IUTAM-Symposium, Sedona, AZ, USA, 1999.

[5] M. Kloker. *Direkte Numerische Simulation des laminar-turbulenten Strömungsumschlages in einer stark verzögerten Grenzschicht.* Dissertation, Universität Stuttgart, 1993.

[6] U. Konzelmann. *Numerische Untersuchungen zur räumlichen Entwicklung dreidimensionaler Wellenpakete in einer Plattengrenzschicht.* Dissertation, Universität Stuttgart, 1990.

[7] U. Rist and H. Fasel. Direct numerical simulation of controlled transition in a flat-plate boundary layer. *J. Fluid Mech.*, 298:211–248, 1995.

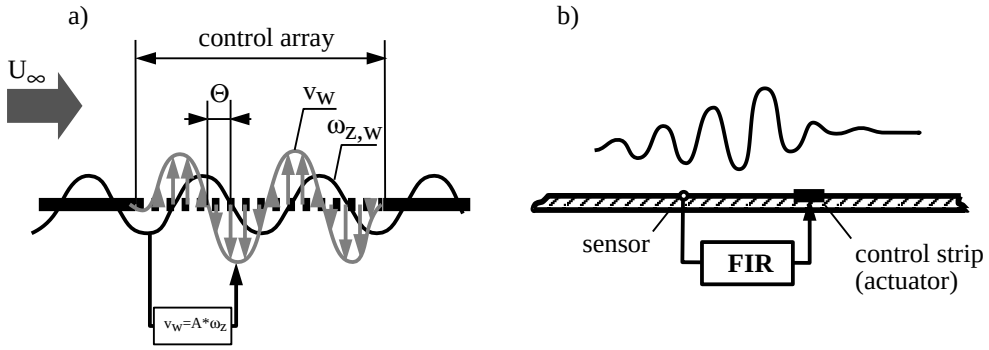

Figure 1: Control principles: a): ω_z-control. b): active control via FIR-filter

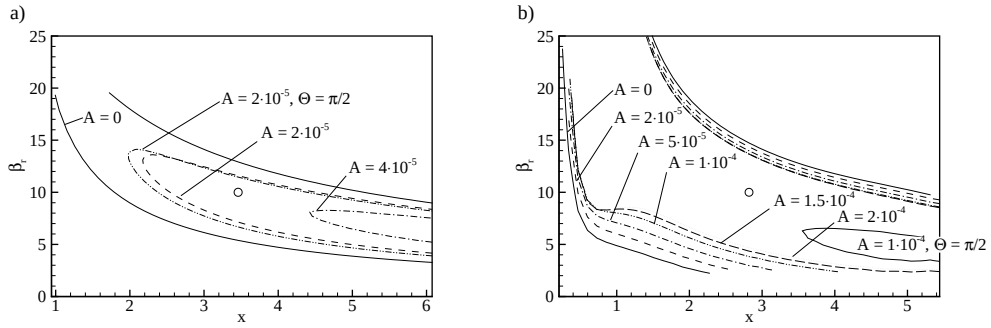

Figure 2: Curves of zero amplification of the investigated base flows.
a): Blasius b): Falkner-Skan base flow with Hartree-parameter $\beta_H = -0.1$. Free stream velocity was $U_\infty = 30\frac{m}{s}$ and x was made dimensionless with $L = 0.05m$. The small circles mark the position in the x/β-diagram of the calculations shown in Fig.3

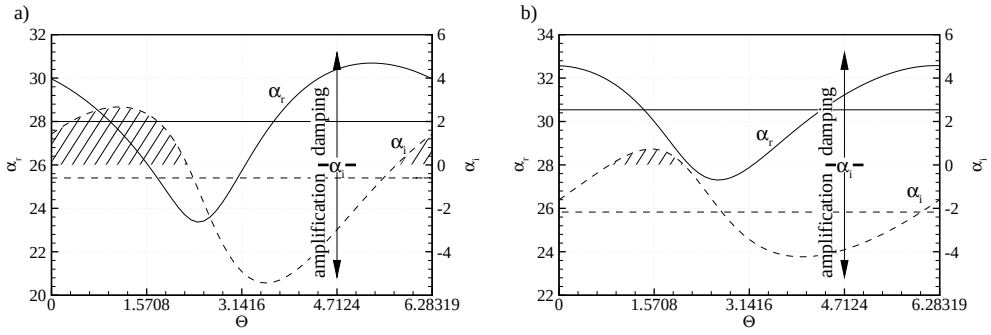

Figure 3: Eigenvalues for a variation of the phase angle Θ between $\omega_{z,w}$ and v_w for a given amplitude-factor of $A = 1 \cdot 10^{-4}$. a): Blasius b): Falkner-Skan. The circles in Fig.2 mark each position in the stability diagram. The horizontal lines (solid and dashed) show the uncontrolled values of α_r and α_i.

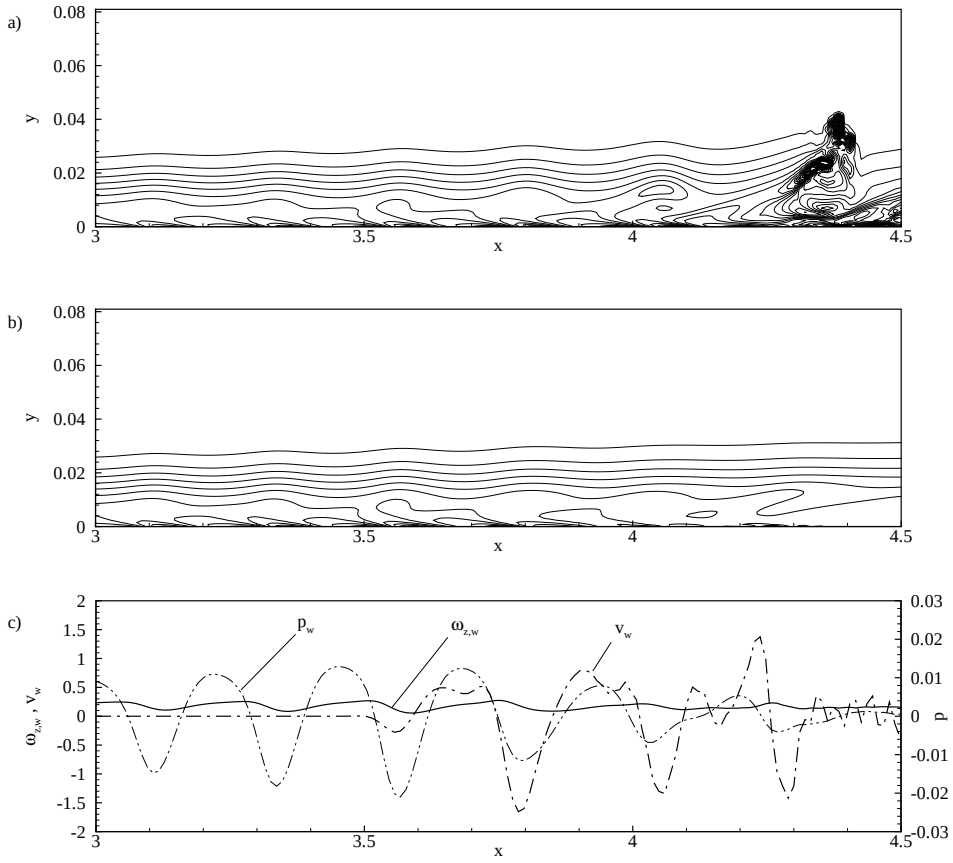

Figure 4: K-breakdown scenario. a): Instantaneous ω_z-iso lines (peak plane) of the uncontrolled case. b): same as (a) but with ω_z-control applied for $x > 3.46$ ($|A| = 2 \cdot 10^{-4}$, optimized phase). c): Distribution of ω_z, v and pressure p at the wall belonging to b).

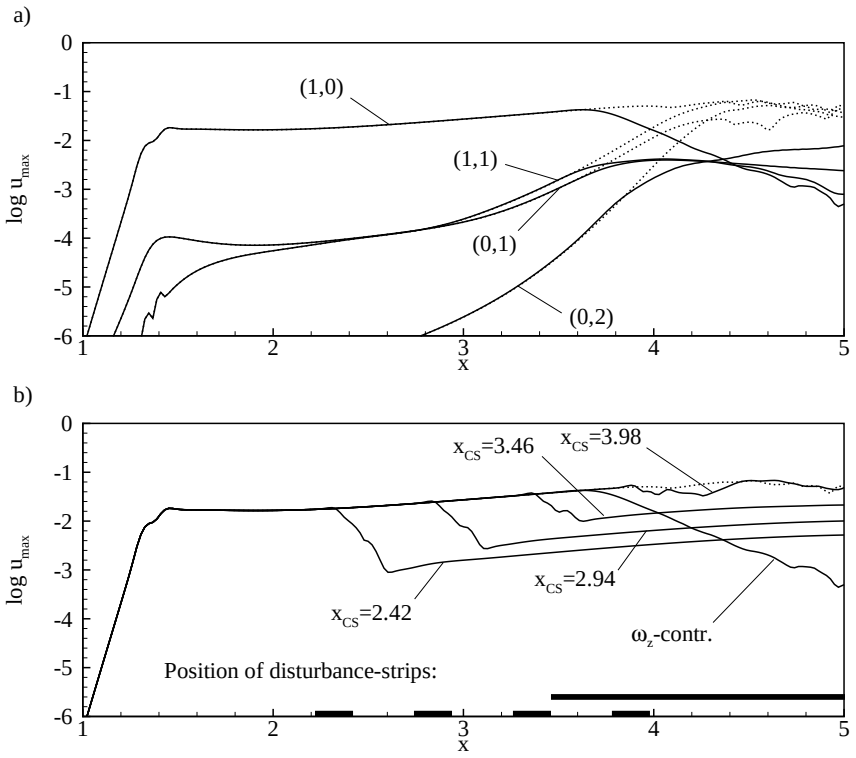

Figure 5: K-breakdown scenario, u_{max}-Amplitudes vs. x. a): Comparison of the most important modes with (solid lines) and without ω_z-control (dotted lines). Control parameters: $A = 2 \cdot 10^{-4}$, $x_{control} > 3.46$, optimized phase b): Same scenario as (a), Modes (1,0) controlled via FIR-filter at four different locations compared to the ω_z-control and the undisturbed case

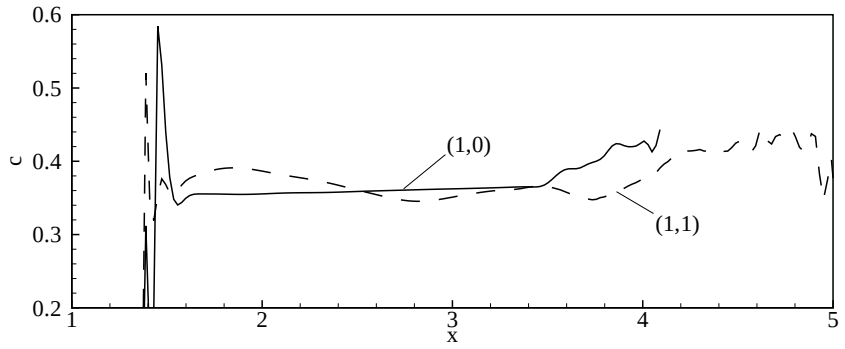

Figure 6: Phase velocities of the resonant modes (1,0) and (1,1). K-breakdown scenario with active control, same control parameters as Fig.5 a)